J Nanostruct 11(1): 1-12, Winter 2021

RESEARCH PAPER

Assembling a Bunch of Transition Metals Oxides on Sodium Montmorillonite Layer for Anionic Polymerization of Butyl Methyl Acrylate

Ameen Abdelrahman[1], Aly M. Radwan[2], A.H. Zaki[3], and Asmaa S. Hamouda[4]

[1] *Department of Renewable Energy Science & Engineering, Faculty of Postgraduate Studies for Advanced Science (PSAS), Beni-Suef University, P.O. Box 62511 Beni-Suef, Egypt*

[2] *National Research Center, Chemical Engineering & Pilot Plant Department, Cairo, Egypt*

[3] *Department of Materials Science and nanotechnology, Faculty of Postgraduate Studies for Advanced Sciences (PSAS), Beni-Suef University, P.O. Box 62511 Beni-Suef, Egypt*

[4] *Department of Environmental Sciences and Industrial Development, Faculty of Postgraduate Studies for Advanced Sciences (PSAS), Beni-Suef University, P.O. Box 62511 Beni-Suef, Egypt*

ARTICLE INFO

Article History:
Received 18 August 2020
Accepted 12 November 2020
Published 01 January 2021

Keywords:
Anionic polymerization
Butyl methacrylate
Clay
Hydrogenation
Spectroscopies characterization
Transition metal oxides

ABSTRACT

In the present study, anionic polymerization of Butyl Methyl acrylate has been carried out in oxygen atmosphere over different heterogenic prepared catalytic systems which are composed of a group of three metal oxides (Ti, Mn Cu) assembled on thin layers of clay (Bentonite) as hydrogenating/ dehydrogenating activation for the polymerization reaction. The prepared catalysts and polymeric products were distinguished by different spectroscopic techniques such as XRD, 1HNMR, energy-dispersive X-ray spectroscopy (EDX), SCN, TEM, IR, and gel permeation chromatography (GPC). we deduced that the dimensions of the efficiency of each catalyst as well as whole composites on the polymerization of Butyl Methyl acrylate of process, also, we approach the reaction mechanism of the polymeric process, furthermore, studying the variation and factors affecting on anionic polymerization like polydispersity index and tactility properties, more details and discussion were deeply investigated blow throughout the analysis and data analysis.

How to cite this article
Abdelrahman A., Radwan A.M., Zaki A.H., Hamouda A.S. Assembling a Bunch of Transition Metals Oxides on Sodium Montmorillonite Layer for Anionic Polymerization of Butyl Methyl Acrylate . J Nanostruct, 2021; 11(1): 1-12. DOI: 10.22052/JNS.2021.01.001

INTRODUCTION

Recently, metal oxides used as efficient heterogeneous catalysts in many organic transformations [1]. Especially in the manufacture of petrochemicals and refining sector, by development catalysts in nano-scale design [2]. Material engineers enable to enhance the catalytic activity of materials using alternative materials in Nano- scales, its lower expensive, eco-environment, nontoxic, easily degradable, and high efficiency. The metal oxide surface is characterized by Lewis acid and base properties, as soon as adding the nature of metal cation and surface area of the metal oxides has extensively magnified their catalytic properties. For instance, Zinc oxide is a low-priced used in nanoscales in various catalytically cracking of organic materials [3-5]. TiO_2 is much more favorable as it is stable, non-toxic, environmentally friendly, plentiful, and cost-effective. Also, MnO_2 is well known as

* *Corresponding Author Email: chem.shaha@gmail.com*

highly catalytic oxidation activity for organics compounds and its good stability with low solubility in supercritical water. [6]. Yu and Savage found that bulk MnO_2 is an active catalyst for the oxidation of acetic acid under supercritical conditions. nanoparticles Metals oxide prepared by various methods to ameliorate their properties and characterize them like good electrical, optical, magnetic properties rather than using bulk counterparts [7].on the other hand, Titania nanoparticles are used in many applications such as optical devices, sensors, and photocatalysis [8,9]. The important factors that should be taken into consideration for the performance of TiO_2 applications are particle size, crystallinity, and morphology [10,11], Furthermore, TiO_2 is strong metal-support interaction, chemical stability, and acid-base property [12]. Utilizing organ-modified clay received much attention since clay layers create a tortuous path against the permeant, yielding better barrier properties, especially for gases [13,14]. Thickness clay is about 1 nm and the side dimensions are around 30 nm to few micrometers, depending on the clay nature and Van der Waals force which is a great effect on interlayer spaces electrostatic forces sheets this force is known as cation exchange capacity (CEC) and is explicit as meq/ 100g. Polymer matrix filled with nano-inorganic particles has been extensively studied, for the easy process and the potential applications as electrical and electronics engineering materials. Especially, the addition of inert inorganic oxides such as SiO_2 Al_2O_3 and TiO_2 [15]. Several techniques have been employed to synthesize nanocomposites: sol-gel, hot pressing of powders, and melt intercalation [16]. In situ polymerization is a straightforward and relatively novel method to produce nanocomposites in which the resin and filler are mixed, cast into a mold, and polymerized [17]. More recently though, researchers have begun to expand the scope of mechanical testing into fatigue, creep, sliding wear resistance, and polishing behavior [18-21]. Many studies have also been run on fracture deportment and toughness of micro-and nano-sized particles embedded in commercial resins.

Today, various organic and inorganic compounds easily improve and modification through different clay activity catalysts [22] such as chemists and scientific researcher worked on clay modification by different materials for instance surfactants in polymerization reaction [23]. Doh and Cho [24], discovered the affinity structural between styrene monomer and modified montmorillonite clay with tetra-alkyl ammonium cations, has a great effect on the final structure and also, Nanocomposites characteristic.it was founded, both metal complexes and metal oxides supported or assembled on bentonite clay promoted the catalytic efficiency in two phases aqueous and bulk polymerization of methylmethacrylate (MMA) with the aid of free radical mechanism [25-28]. Lately, studies propose an impact for particle size and metal oxide surface area (SiO_2, Al_2O_3, TiO_2 and CeO_2) in free radical MMA polymerization [27]. Solyman et al, confirmed throughout their research on polymerization of MMA that free radicals were reduced by oxygen in presence of CuO/TiO_2 in addition to, augment the polymerization of MMA reaction via the redox-initiated mechanism. Also, other studies confirmed the important role of oxygen deactivated the polymerization reaction in case CuO/clay and no changeable reaction by using CoPc/clay.

Poly(n-butyl acrylate) is one of the industrially applicable polymers because it has low glass-transition temperature, durability, and potential impact like a soft segment in elastomers thermoplastic. Generally, conventional free-radical polymerization is the best methods for preparing Poly(n-butyl acrylate)) which is without microstructure control. So in the present work, it is seek to focal point on prepared catalyst act used addition to polymerization techniques also provide an easier way to create polymers with predetermined molecular weight and narrow poly dispersities[[26] polymerization has been successfully used to make n-butyl acrylate (nBA) homopolymer and block copolymers [31]. Some studies have been done on copolymers of butyl methyl methacrylate and blend of poly Bu- MMA, [32] but in another view nano metal (TiO_2) is widely used in the many applications of photodegradation rate of polymers with excellent results. In this study, it was prepared and characterization of metals oxides using different spectroscopic techniques rather than assembled of metals oxide on Bentonite clay with characterize and applicable of nano-composite materials on anionic polymerization Butyl Methacrylate Polymer (BuMMA) in the presence of oxygen using GPC and ^{1}H NMR characterization.

MATERIAL AND METHODS

Catalyst preparation

All chemicals which used for nano-oxide metals were purchased from Loba cheme (India) and were used without purification. The manganese oxide (MnO_2) nanoparticles were prepared using the co-precipitation method. Two different anions, manganese (II) sulfate, and manganese oxalate salts were used for the preparation. The same quantity of both slats with 0.2M concentration are mixed with continuous stirring (about 1 hour) at a constant temperature of 60 °C. During stirring add sodium hydroxide solution till getting pH 12. To obtain brown precipitates, then filtered and washed two times with ethanol. Dehydrated it overnight at 100°C then preserved in the oven at 500 °C for 5 hours. Titanium oxide (TiO_2) NP was got ready by the physical grinding method by physical grinding method. A quantity of 100 gm TiO_2 powder came in a grinding machine that has a high-speed rotator. It was uniformly ground and crushed well for 15 min with utmost precaution to avoid any contamination. In the end, the finely ground powder was separated to get nano-size powder TiO_2 which was packed in plastic pouches and stored at normal room temperature until use. Zinc oxide (ZnO) nanoparticles were produced by using the sol-gel method. In a typical procedure, 12.6g of zinc acetate dehydrate was added to 400 ml of double-distilled water. The mixture is stirring continuously to dissolve zinc acetate completely. Then the obtained solution was heated till 50 °C, by adding 600 ml slowly and stirring for 30 min. Then followed by dropped of 6 ml of H_2O_2 (47%) the mixture carefully and mixed it using a magnetic stirrer to get an almost clear solution. This solution was incubated for 24 hours and then was dried at 80°C for several hours to obtain white zinc oxide nanoparticles. Zinc oxide nanoparticles was washed several times by distilled water to flit the by-products. After washing, the ZnO nanoparticles were dried at 80 °C in a hot air oven to obtain the complete conversion of zinc [27].

Clay (Bentonite powder) was purchased from M-I SWACO, Egypt. The clay nanopowder was prepared using RETSCH Planetary Ball Mills Type PM 400. The sample clay was crush using the ball mill with a speed of 150 rpm for 8 hours.

Each nano-composite (ZnO, TiO_2, and MnO_2) were prepared by simple impregnation method as shown in Fig. 1. One gram of Bentonite nanoparticles was dispersed in 250ml of water then 0.5g of each metal oxide was added to prepare the desired composite. The TiO_2-Bentonite, MnO-Bentonite, and ZnO-Bentonite nanocomposites were then filtered and washed several times with distilled water. Samples were dried overnight at 100 °C and then applied physical grinding method to enable size reduction. In brief, a quantity of 100g each composite was put in a grinding machine which having high speed rotator for 10 h.

RESULT AND DISCUSSION

Characterization of the composite catalyst

XRD characterization

Fig. 2 shows the XRD pattern of the Bentonite

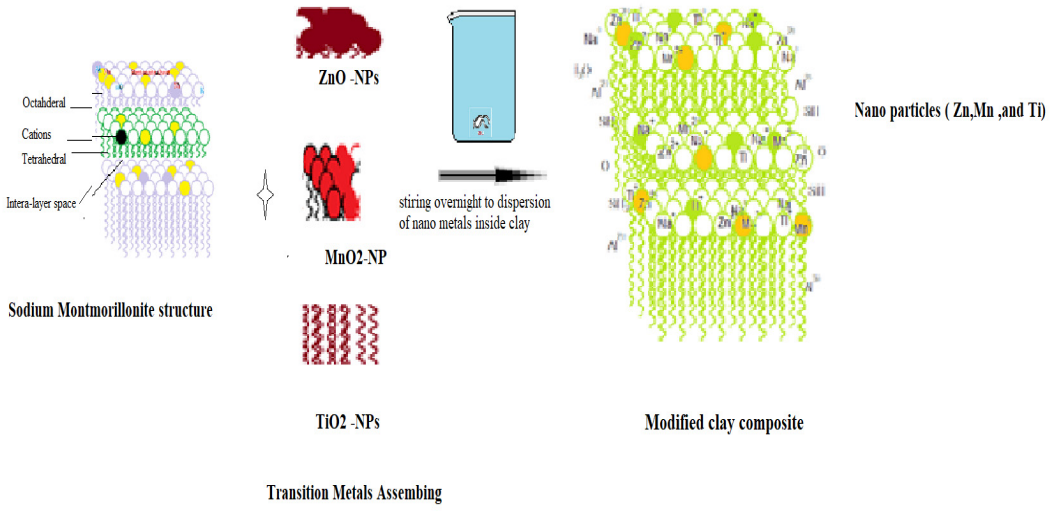

Fig. 1. Schematic diagram for the impregnated process of metal oxides with Bentonite.

Table 1. Peak positions (2**θ degree) of XRD patterns clay and different metal oxides.**

Material	Peak position (2θ, degree)
MnO_2	18.18, 37.48, 42.82, 58.81, 6.21,74.58 and 78.43
Bentonite	6.80, 12.26, 19.80, 20.81, 24.85, 26.64, 35.11, 36.57, 50.16, 54.80, 61.72 and 68.07
TiO_2	25.34, 37.00, 37.85, 38.63, 48.09, 53.96, 55.13, 62.73, 68.79, 70.40 and 75.14
ZnO	20.57, 26.72, 31.84, 34.51, 36.32, 47.62, 56.67, 62.93,66.49, 68.02, 69.17 and 77.05

(clay), MnO_2, ZnO, TiO_2, and their composites. Table 1. lists the peaks of ICDD cards for all the samples under study. By comparing the data between the XRD pattern in the figure with ICDD data previous table, TiO_2 Np and prepared MnO and ZnO display a good covenant between them. Through XRD data it appears the oxides state a is high crystallinity with calculating average particle size (d) of metals oxides and their strong intensity peak using the Debye-Scherrer equation as

$$d = K\lambda / B \cos(\theta). \quad (1)$$

Where K is the Scherrer constant (0.89), λ is the wavelength of streak rays used, B is equal to the entire width at semi maximum (FWHM) of diffraction (in radians) and θ is the Bragg's angle. As clear from Fig. 2b, MnO_2 metal nanoparticles synthesized were crystalline. The average particle size of MnO_2 nanoparticles was around between 20-35 nm where the intensity of the main MnO_2 lines sharply increased, furthermore, the appearance of new packs at 2θ angles: 18°, 38°, 43°, and 63°. For ZnO nanoparticles [Fig. 2C], X-ray diffraction display metal oxide is ZnO is characterized by hexagonal structure and no peak turns into visible due to others material fasten to its phase point out a high degree of purity prepared sample. The widen X-ray diffraction lines throwback the nature nanoparticle of the sample. By focus, it is observable that the intensity of the peaks be seen marvels crystal growth of the oxide Nanoparticles. The calculated average crystallite is 45 nm attached with the surface area of ZnO nanoparticles is 4.3737 m^2/g. The intensity of the main TiO_2 lines sharply increased, in addition to the appearance of new lines at 2θ angles: 21°, 25.5°, 27°, 38°, 57° and 63° as clear in Fig. 2d. The X-ray pattern reflected that the TiO_2 is very pure and consists of a majority of anatase particles. Concerning Fig. 2d it is provided the list peaks set up powder diagrams gave us the average crystallite size is 25 nm and the surface area of TiO_2 nanoparticles is 60 m^2/g.

XRD patterns of MnO-Bentonite, ZnO-Bentonite, and TiO_2-Bentonite nanocomposites [Fig. 2 e, f, and g] confirmed the preparation of the desired catalysts, where the patterns showed mixed peaks of Bentonite and metal oxides. It is worth mentioning that, in the case of TiO_2-Bentonite and ZnO-Bentonite nanocomposites, the peaks of TiO_2 and ZnO are predominant in the patterns which may be attributed to the good distribution of TiO_2 and ZnO on the Bentonite-surface. For the ZnO-Bentonite, new diffraction lines with high intensity appeared which are characteristic of the ZnO phase (ASTM 05-0664). In addition, the lamella line of the Bentonite was shifted to the left (to a higher d-spacing), which reveal the perforation of ZnO inside the Bentonite lamella resulting in this expansion.

Fig. 3 (a-d) shows the TEM micrographs of Bentonite, MnO_2/Bentonite ZnO/Bentonite, and TiO_2/Bentonite nanocomposites, respectively. It is clear from Fig. 4 (a) that, the average particle size of natural Bentonite exceeded 100 nm with no uniform shape. The MnO_2- and ZnO nanoparticles are deposited on the Bentonite surface (Fig. 4b and Fig. 4c) while the TiO_2 nanoparticles uniformly covered the Bentonite surface, Fig. 4 d. Due to this uniform coverage, the XRD patterns of pure TiO_2 and TiO_2-Bentonite are very close to each other. Since a can be defined by studying of crystallite orientation of the lattice edges, one can see the mean crystallite size in the synthesized TiO2 crush is about 10~15 nm in diameter. As a main functional metal oxide, MnO_2 nanoparticles are one of the most attractive inorganic materials because of their physical and chemical properties and wide applications in catalysis, ion exchange, and molecular adsorption. It is clear from Fig. 4b that the average size of MnO_2 is about 25-30 nm. There are large numbers of potential applications of MnO_2 nanoparticles such as catalysis application in cracking of polyolefin and petroleum refinery industrial. On the other hand, the size of ZnO-Bentonite nanoparticles is about 27-82 nm as shown in Fig. 3c.

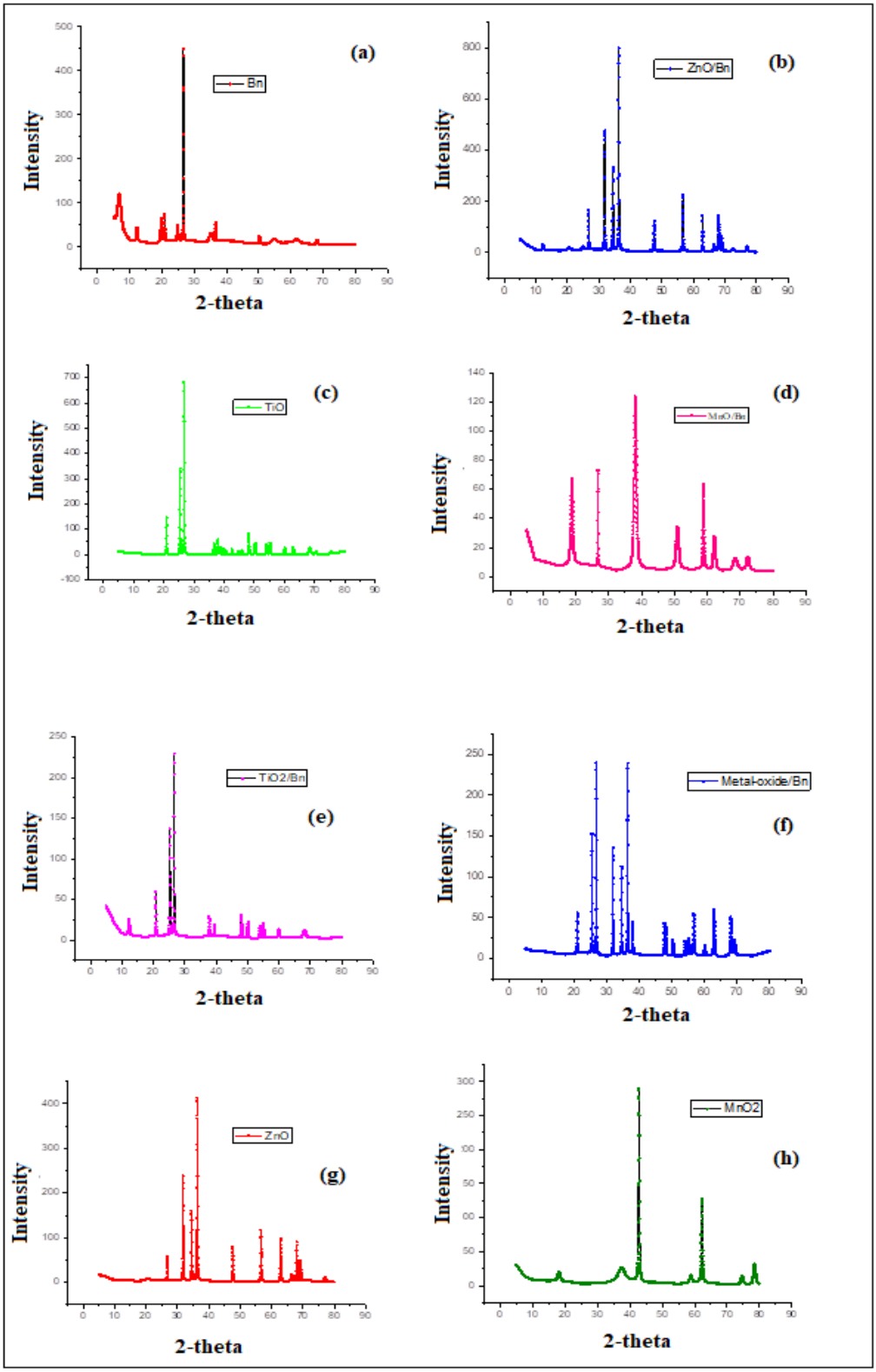

Fig. 2. XRD pattern of the samples under study

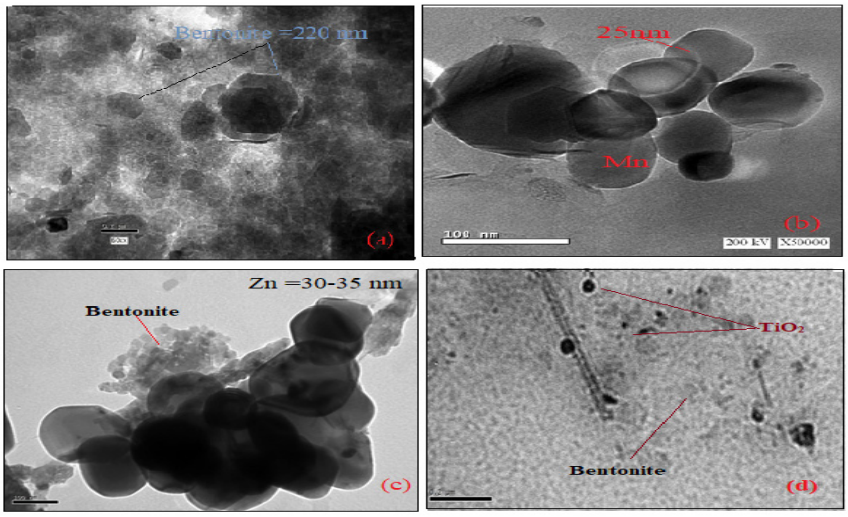

Fig. 3. TEM micrograph of (A) pure natural Bentonite, (B) MnO-Bentonite, (C) ZnO-Bentonite, and (D) TiO_2-Bentonite nanocomposites.

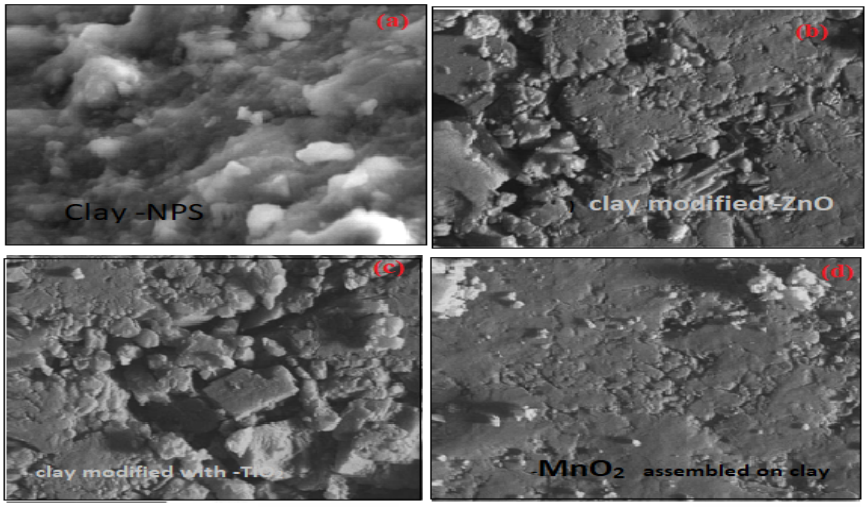

Fig. 4. SEM images of the clay Nano powder (b) ZnO-Bentonite, (c) SEM of TiO_2-Bentonite nanocomposites (d) SEM of MnO-BN.

The SEM technique was used to investigate the surface morphologies of the prepared samples. The surface morphologies of the clay nanopowder, the fabricated clay nanocomposite with (ZnO, MnO_2, and TiO_2) are shown in Fig. 4. The structure of the clay nano-powder and the fabricated Metals clay nanocomposite are indicated in Fig. 4a and Fig. 4b shows a massive layered structure with some large flakes and some inter-layer spaces. A comparison between the SEM images in Fig. 4c and Fig. 4d, it is noticed that nearly the same surface morphologies with the exception that the interlayer spaces are decreased in Fig. 4a. This is maybe related to the impregnation of the metal oxides between the clay layers. It is noticed that the inter-layer spaces are more decreased in Fig. 4c and Fig. 4d which indicate the impregnation of the nanostructure of the metals oxides between the clay layers.

Studying the activity of prepared nano-composites /Metals oxides as the catalyst on polymerization (BuMMA).

The performance of clay composite metals oxides catalysts was evaluated in the bulk polymerization of the Butyl Methacrylate reaction. The new distilled stabilizer-free monomer (B-MMA) Butyl Methacrylate was prepared by agitated with

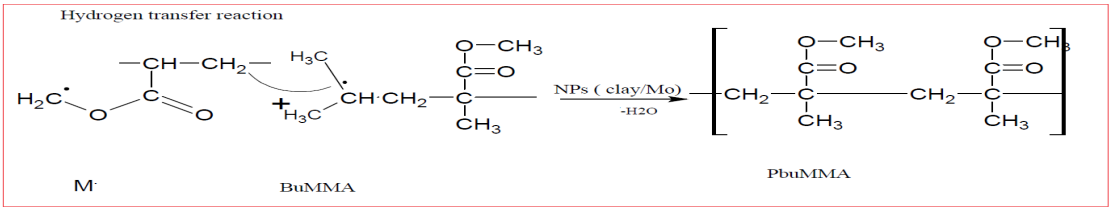

20% NaOH solution get rid of Quinone inhibitor, distilled water washed several times, one time with ammonium acetate to neutralize. Then was dried over $CaCl_2$, vacuum distilled and stored at about 6 ◦C anhydrous sodium sulfate [30]

The freshly distilled stabilizer-free monomer (2.8 g) was introduced into the Butyl Methacrylate polymerization tube (20 ml capacity) together with 0.06 g of each modified clay sample. The reaction mixture was de-aerated by pure dry nitrogen and then the reaction tube was sealed and set down inside thermo-stated water bath regulate at 80 ◦C, for 6 h. the same process of polymerization reaction was repeated by replacing pure and dry O_2 instead of N_2 using the same catalyst samples, to explore reaction mechanism. Cooling to room temperature, then opened the tube carefully with dissolving the product in acetone, shaking, filtered to separate the catalyst and the filtrate was run in methanol to precipitate the polymer (10:1 ml of alcohol the reaction mixture). The produced polymer was filtered and dried under vacuum at 40 ◦C till consistent weight.

Fig. 5 Preparation Butyl Methacrylate polymer in ionic liquid by composite Metals oxides and clay Manganese based on catalysts has not been widely studied for the condensation of organic compounds like butyl methacrylate l, being most of these research and studies of homogeneously catalyzed were recorded as previous literature reviewer Ghaziaskar et al. [33] is one of fewer scientists carried out dehydrogenation on organic compounds like ethanol in existence Mn2O3 and nickel propped over alumina inside the fixed-bed reactor to get a high quantity of ethanol conversion of 18.7% at 523. Also, surface catalyst engineering was applied different species of catalyst MgAlO mixed oxide catalysts (M=Pd, Ag, Mn, Fe, Cu, Sm, Yb) on biohazard autoclave conversion at 473 K with M). on the other hand, in recent studies, TiO_2 used as a supported for Ni-Mn catalysts to explore rebuilding carbon bonding structure, for instance, in synergy energy application of CO_2 and CO by hydrogenation activity in our mechanism, it is tried to approach by the redistributed interface between transition metals (TI, MN, and Zn) which they are stable energy level (d-orbital equal 0 or empty valence,7 or half shell and 14 or full with electrons) respectively that is clear the most reactive metal is Mn metal to make stable chelating or cluster complex with a carbon chain of polymeric as a wall, cation exchange of cations and anions on clay thin layer, then it will set up active sites for Carbon and Oxygen by replacing them to get rid of one molecule of H_2O. Another explanation could be back to the strong interaction between Mn and Ti as a metallic bond, an important part for the composite catalyst to promoter nanoparticles metals (Ti, Mn, and Zn) and other cations on the clay sheet by forming redox-oxidation process which leads to anionic polymerization of butyl methacrylate.

The polymer yield (% conversion) was calculated as follows:

$$\text{Polymer yield}\left(\text{Y}\%\right)=\frac{\text{weight of produced polymer}}{\text{weight of monomer}}\times 100$$

Characterization of Butyl Methacrylate Polymer (BuMMA).

Fourier transform infrared spectrometer (FTIR)

All spectra were done by using the Fourier Transform Infrared, (ATI Mattson genesis and FTIR) at 2 cm^{-1} resolution .the infrared spectroscopic analysis of the prepared polymeric was conducted by the Egyptian Petroleum Research Institute.

From IR many spectrum bands were observable that appear in Fig. 6 starting by low wavelength the vibration appears at 750 cm^{-1} and 872 cm^{-1} residuals of transition atoms (TI, Mn, or Zn) of nano composite catalyst. The broad peak around 3400 cm^{-1} and 3600 cm^{-1} is a good inductor for the hydroxyl group of prepared polymers. there is another strong peak stretching between 1646.6 and 1731 cm^{-1}, which is evidence for carbonyl group C=O functional group like CH_2, vibrated

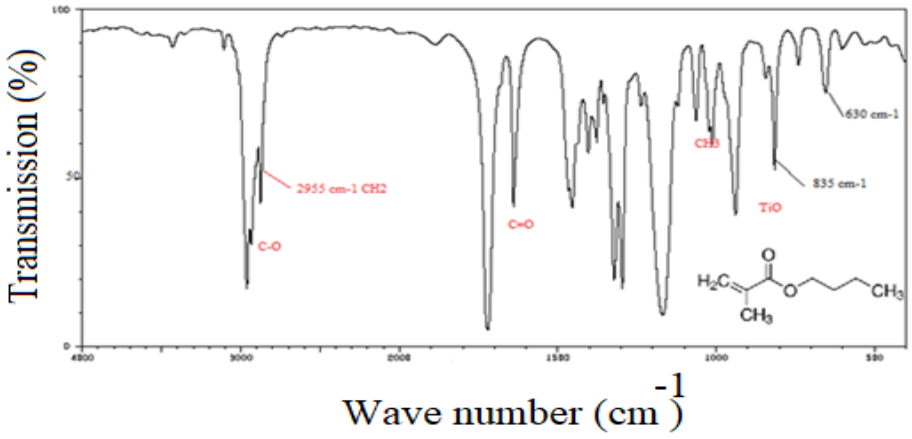

Fig. 6. FTIR-spectrum of PBuMMA

Table 2. summarized An ionic polymerization of poly Bu- MMA by modified composites catalysts in presence of O_2 and N_2 Atmosphere .

Catalyst	% BMMA in presence of N2	% BMMA in presence of O2	β	α	Mw(x 10^{-5})	Mw/Mn	tactility specificity ratios			
							S(rr)	H(mr)	I(mm)	pentads
Bentonite no additives	0	0.09	0.46	3.21	1.91	1.55	54.7	32.6	2.5	3.6
Composites ZnO/ Bn	1.5	7.0	3.02	4.28	7.84	1.42	52.1	24.7	10.7	8.7
CompositesTiO2 / Bn	4.3	38.2	0.44	2.53	3.01	2.6	55.0	33.0	2.6	11.3
CompositesMnO2/ Bn	5.6	79.8	0.53	3.53	2.19	1.06	59.8	34.9	2.9	10.8

at 2955 and 3000 cm^{-1}. Also, methyl group carbon Skelton CH_3 has a strong peak around 1140 1194 and 1240 cm^{-1}. on the other hand, symmetry (CH_2) at 2850 cm^{-1}, ν asymmetry (CH_2) at 2925 cm^{-1}, , ν (C=C) 1 for acrylic group at 1560 cm1,δ (CH_2) bending at 1455 cm^{-1}, ν asym (COC) at 1250 cm^{-1}, ν sym (COC) at 1045 cm^{-1}. By comparison of getting data from H-NMR and IR data analysis, it can be confirmed composites clay catalyst is successful in the polymerization process.

Energy-dispersive X-ray spectroscopy (EDX)

The Energy Dispersive X-ray Analysis (EDXA) was used to investigate the main composition of the prepared sample, which contain metals cations like Na, Ca, Mg, and assembled transition metals samples (Mn, Zn, and Ti), as well as clay composition (silicate and aluminate).
This analysis is a good indication of impregnated bentonite clay by three metals and also confirms the XRD and TEM analysis.

Elucidation effecting of composites catalysts on BuMMA polymerization process.

Through analysis of weight distribution produced polymers which implement by gel permeation chromatography (GPC). Measurements were performed in toluene of HPLC by using grade as a mobile phase has elution, 0.7 ml/min at 40 ◦C. Molecular weights were detected relative to monodisperse polystyrene standards. Calculations were done by the Millennium 32 Chromatography Manager and gel-permeation application software.

Butyl Methacrylate Polymer (BuMMA) analysis was done via proton nuclear magnetic resonance spectroscopy (^{1}H NMR) which acquire by a Bruker-300 MHz spectrometer superconducting magnet and 5 mm dual-probe head. The solvent used is $CDCl_3$ and tetramethyl silane as an internal reference. The results of bulk polymerization of Butyl Methacrylate Polymer (BuMMA) carried out at 80°C for 6h in N_2 and O_2 atmosphere were summed up in Table 2. In our test, the catalyst–monomer ratio was 2.4 % (0.06 g of weighted catalyst to 2.8 g of catalyst used as monomer). The % cracked of Butyl Methacrylate in nitrogen and oxygen atmosphere by using nano-clay is zero. Whereas the % conversion of in Nitrogen atmosphere in case nano-clay composite with the polymer is also zero, it is slightly increased to 0.09% in O_2 atmosphere. While using the nano clay composites with Zn, Ti, and Mn metals oxides, it is noticed that, by comparing the increase in

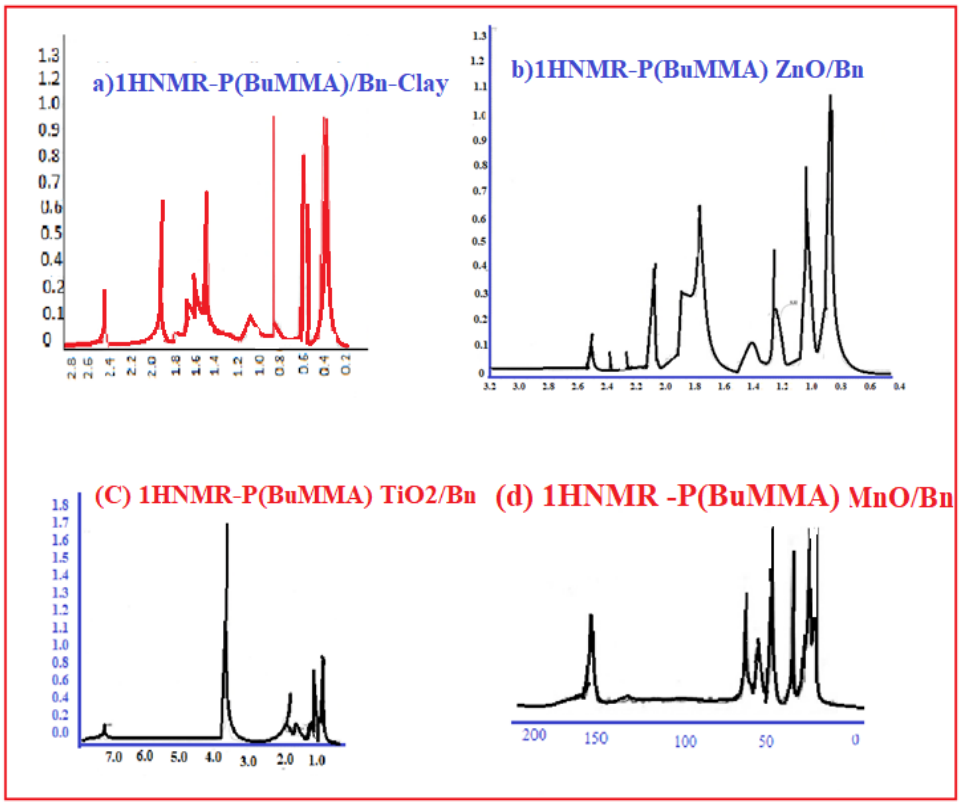

Fig. 7(a-d) .1HNMR-spectrum of created Butyl Methacrylate

case O_2 and N_2, the conversion % increased from 0.09,7,38.2 and 79.8 to 0,1.5,4.3 and 5.6 respectively according to the below Table 2. The augmentation of catalytic activity may be linked with the possible activation of clay active sites mainly OH groups. Also, it might be acceptable that the metal nanoparticles penetrate in between layers of clay and set up new active sites through functional groups activated by oxygen followed by promoting the polymerization process via an anionic mechanism. In addition to using the composites Nano-clay (Zn, Ti, and Mn) metals oxides, the act created new sites by making bond (H bond) through free electron in the d-Orbitals shell. That resulted in delamination of clay layers as shown from TEM micrographs Fig. 3 (a-d). That confirms by actuality a creation and exposing new active sites clay layers, mainly hydroxyl groups which is the main reason for increasing the catalytic activity and thus the % conversion up to 5.6 % using Mn -Bn as an example in N_2 atmosphere. Most probably, these active sites highly activated in the O_2 atmosphere, so the % conversion increased up to 79.8 % using Mn -Bn composite sample.

the polydispersity index (Mw/Mn) linked with the nature of growing chains and their distribution on the surface active sites, and the tact specificity values of the formed polymers (from ^{1}H NMR measurements as shown Fig. 7 (a-d) for the Nano-clay composite, Bentonite composites with ZnO, TiO_2. Table 2 shows that the αw value of Butyl Methacrylate Polymer slightly increased by using nano Bentonite composite with ZnO relative to the Bentonite composite with correlate with inappreciable increasing of polydispersity index (Mw/Mn =1.06). This prof that the pervious -mentioned of result that assembled polymer around Bentonite nanoparticles in ZnO sample that promotes more active sites which initiated by oxygen lead to increasing the % conversion and the value of Mw.

On the other hand, decreasing in Mw values for Butyl Methacrylate Polymer by using the nano Bentonite composites (TiO_2 and MnO_2) confirms further creation of active conjugate resulted in an obvious increase in % conversion comparing to decreasing in αw values, increase in αn, and

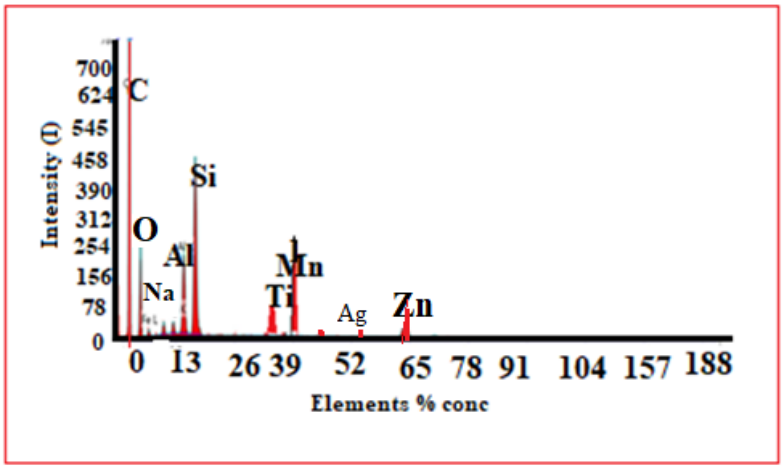

Fig. 8. EDAX for gasified char sample

thus low polydispersity, referred to the Table 2. The optimum catalyst sample is Bentonite -MnO_2which provide, the best performance of catalytic polymerization of Bu- MMA both of increasing 79.8 % conversion and polydispersity index mean, it is closer to 1 relative to the others. This indication of the suitable ability of this new catalyst work as heterogeneous performance in polymerization Butyl Methacrylate Polymer.

By noticing the increasing number-average molecular weight, that means, it is a good indicator of free radicals oxygen in case composite clay –MnO_2, this free-radical helps in initiation and propagation process, thus increasing in conversion. To compare to samples (composite clay-TiO_2 & Composite Bentonite –ZnO) which are drastically decreasing.

Both the polymerization rate and the conversion % increase with a strong decrease of the Mw, which means more control using MnO_2/ Clay .so, the best polydispersity index (Mw/Mn = 1.06). In addition, the glass effects mostly appear with high conversion. Conversion (%) decreases the Mw and Mn values.

The mechanism of created Polymer by using composites catalyst

Mention to Table 2. it is clear that the polymers produced using all catalyst samples show prevailing syndiotactic structures. This reflects that **poly Bu-MMA** bulk polymerization has occurred via a free radical mechanism in presence of oxygen. The iso tactility of polymer was changed from 2.5 to 10.7, 2.6, and 2.9 when utilizing nanoparticles clay and the nano Bentonite composites with ZnO, TiO_2, and MnO_2 samples respectively. This sort of monomer unit's arrangement is demonstrated as the free radical mechanism, due to the main reason for the presence of O_2. Furthermore, that kind of polymerization **poly Bu-MMA** is the anionic mechanism, because it was done without using an initiator or co-catalyst. By studying The pentads (mmmr or rmmr appeared at 1.21 ppm in the ^{1}H NMR spectra. which confirms exists of new deep active sites although, decreasing with a large extent by using MnO2- Bentonite sample surely due to complete clay layers delamination. the polymer isotacticity (mm triads) changed from 2.5 to 10.7, 2.6, and 2.9 by using ZnO, TiO_2, and MnO_2 samples respectively. This behavior in the monomer unit's arrangement confirms that bulk polymerization of MMA mostly proceeded through by free radical mechanism is initiated stage via O_2 and more exposed OH−groups As impact by the following equation: 4[mm][rr]/[mr]^2. The β values of syndiotactic polymers created in all cases are close to 1 except the Bentonite composite with ZnO-sample, indicating most probably the chain–end control mechanism according to the activity of using Bentonite composite < nano Bentonite / ZnO < composites Bentonite -TiO_2 < Bentonite -MnO_2 polymers samples. Also, the α values (According to equation:2[rr]/[mr]) of the novel polymers **of Bu-MMA** are noticed far from 1, this means no enantiomorphic–site control approach. All in all, that record is most likely catalyst-controlled, i.e., the process gets more controlled due to, the density of the surface-active sites increases by

delamination of clay layers especially using the Bentonite -MnO_2 sample.

CONCLUSION

Throughout this paper, it is reported on preparation and characterization of a new hetero catalyst which provides good results in bulk polymerization (ionic polymerization) by activated hydroxyl group to free radicals and initiated the polymeric process, furthermore, ion exchange (clay layers) make a chelating complex with metals (Mn^{+2}) through by free empty electron in d- shell and the surface area of other metals (Zn, Ti^{+2}). Thus, this composite is more existence, green environmental, and less expensive than other catalysts using in the industrial field. It is strongly recommended to uses in the petrochemicals industrial sector. On the other hand, geopolymer clay (Bentonite) has great activity especially in catalytically cracking, that is what was happened by modified its characteristic, to get better results in our application of (**poly Bu-MMA)** Butyl Methacrylate polymerization. As well as it is going to use as a hetero-catalyst in different petrochemicals and refining process industries, furthermore,it has unique properties like as a green material, easily recyclable, nontoxic, and cheap compare catalyst cost . Modified clay metals catalyst has been worked on an ionic mechanism on the reaction of polymer. This is due to the electron orbitals theory of transition metals which it is facilities the electrons transfer in different outer orbitals, complexes forming. Overall Bentonite clay in past in decomposition polymeric carbon chain, but in this research polymeric materials were created by modified clay.

CONFLICT OF INTEREST

The authors declare that there is no conflict of interests regarding the publication of this manuscript.

REFERENCES

1. Bandyopadhyay P, Sathe M, Prasad GK, Sharma P, Kaushik MP. Mesoporous mixed metal oxide nanocrystals: Efficient and recyclable heterogeneous catalysts for the synthesis of 1,2-disubstituted benzimidazoles and 2-substituted benzothiazoles. J Mol Catal A: Chem. 2011;341(1-2):77-82.
2. Anumol EA, Kundu P, Deshpande PA, Madras G, Ravishankar N. New Insights into Selective Heterogeneous Nucleation of Metal Nanoparticles on Oxides by Microwave-Assisted Reduction: Rapid Synthesis of High-Activity Supported Catalysts. ACS Nano. 2011;5(10):8049-8061.
3. Sarvari MH, Sharghi H. Reactions on a Solid Surface. A Simple, Economical and Efficient Friedel–Crafts Acylation Reaction over Zinc Oxide (ZnO) as a New Catalyst. The Journal of Organic Chemistry. 2004;69(20):6953-6956.
4. Goharshadi EK, Ding Y, Nancarrow P. Green synthesis of ZnO nanoparticles in a room-temperature ionic liquid 1-ethyl-3-methylimidazolium bis(trifluoromethylsulfonyl) imide. Journal of Physics and Chemistry of Solids. 2008;69(8):2057-2060.
5. Moghaddam FM, Saeidian H. Controlled microwave-assisted synthesis of ZnO nanopowder and its catalytic activity for O-acylation of alcohol and phenol. Materials Science and Engineering: B. 2007;139(2-3):265-269.
6. Paul DR. Ind. Eng. Chem. Res. Goes Biweekly. Ind Eng Chem Res. 2001;40(1):16-16.
7. Xu H, Wang X, Zhang L. Selective preparation of nanorods and micro-octahedrons of Fe_2O_3 and their catalytic performances for thermal decomposition of ammonium perchlorate. Powder Technol. 2008;185(2):176-180.
8. Harizanov O, Harizanova A. Development and investigation of sol–gel solutions for the formation of TiO_2 coatings. Sol Energy Mater Sol Cells. 2000;63(2):185-195.
9. Tian Y-Z, Li Y-L, Wang Z-F, Jiang Y. Nuclease-responsive DNA–PEI hollow microcapsules for bio-stimuli controlled release. J Mater Chem B. 2014;2(12):1667-1672.
10. Behnajady MA, Modirshahla N, Shokri M, Elham H, Zeininezhad A. The effect of particle size and crystal structure of titanium dioxide nanoparticles on the photocatalytic properties. Journal of Environmental Science and Health, Part A. 2008;43(5):460-467.
11. Lee K-M, Suryanarayanan V, Ho K-C. Influences of different TiO_2 morphologies and solvents on the photovoltaic performance of dye-sensitized solar cells. Journal of Power Sources. 2009;188(2):635-641.
12. Bagheri S, Muhd Julkapli N, Bee Abd Hamid S. Titanium Dioxide as a Catalyst Support in Heterogeneous Catalysis. The Scientific World Journal. 2014;2014:1-21.
13. Sinha Ray S, Okamoto M. Polymer/layered silicate nanocomposites: a review from preparation to processing. Progress in Polymer Science. 2003;28(11):1539-641.
14. Zhang M, Sundararaj U. Thermal, Rheological, and Mechanical Behaviors of LLDPE/PEMA/Clay Nanocomposites: Effect of Interaction Between Polymer, Compatibilizer, and Nanofiller. Macromolecular Materials and Engineering. 2006;291(6):697-706.
15. C.C. Chang, W.C. Chen, Chem. Mater. 14 (2002) 4242.
Chang C-C, Chen W-C. Synthesis and Optical Properties of Polyimide-Silica Hybrid Thin Films. Chem Mater. 2002;14(10):4242-4248.
16. Hussain M, Nakahira A, Nishijima S, Niihara K. Fracture behavior and fracture toughness of particulate filled epoxy composites. Materials Letters. 1996;27(1-2):21-25.
17. Singh RP, Zhang M, Chan D. JMatS. 2002;37(4):781-788.
18. Ng CB, Ash BJ, Schadler LS, Siegel RW. A Study of the Mechanical and Permeability Properties of Nano- and Micron-TiO_2 Filled Epoxy Composites. AdCoL. 2001;10(3):096369350101000.
19. Rodríguez J, Martín A, Pastor JY, Llorca J, Bartolomé JF, Moya JS. Sliding Wear of Alumina/Silicon Carbide Nanocomposites. J Am Ceram Soc. 2004;82(8):2252-2254.
20. Parsons M, Stepanov EV, Hiltner A, Baer E. JMatS. 2000;35(8):1857-1866.
21. Kara H, Roberts SG. Polishing Behavior and Surface Quality

of Alumina and Alumina/Silicon Carbide Nanocomposites. J Am Ceram Soc. 2004;83(5):1219-1225.
22. Doh JG, Cho I. Synthesis and properties of polystyrene-organoammonium montmorillonite hybrid. Polym Bull. 1998;41(5):511-518.
23. Zhu J, Morgan AB, Lamelas FJ, Wilkie CA. Fire Properties of Polystyrene−Clay Nanocomposites. Chem Mater. 2001;13(10):3774-3780.
24. Hassan SA, Yehia FZ, Hamed AA, Zahran AA, Solyman SM. Interaction characteristics controlling catalytic performances of Ni (II) and Cu (II) phthalocyanines immobilized on bentonite clay surface in redox-initiated polymerization of methyl methacrylate in aqueous medium. Journal of Porous Materials. 2010;18(1):1-11.
25. Solyman SM, Hassan SA, Sadek SA, Abdel-Samad HS. Redox-Initiated Bulk Polymerization of Methyl Methacrylate Using a CuO/TiO_2 Catalyst System. International Journal of Polymeric Materials. 2010;59(7):475-487.
26. Sadek SA, Solyman SM, Abdel-Samad HS, Hassan SA. Catalytic Behavior of Cobalt (II) Phthalocyanine Immobilized on Bentonite Clay in Bulk Polymerization of Methyl Methacrylate. International Journal of Polymeric Materials. 2010;59(5):353-369.
27. Zhang H, Van Der Linde R. Atom transfer radical polymerization ofn-butyl acrylate catalyzed by CuBr/N-(n-hexyl)-2-pyridylmethanimine. J Polym Sci, Part A: Polym Chem. 2002;40(21):3549-3561.
28. Contents: Macromol. React. Eng. 11/2014. Macromolecular Reaction Engineering. 2014;8(11):739-740.
29. Li J, Sun Z, Zhen Y, Ren Q, Yu Q, Cui Y, et al. Characterization of poly(butyl acrylate) diols prepared via atom transfer radical polymerization and subsequent modification. Journal of Polymer Research. 2009;17(4):551-556.
30. Yin M, Habicher WD, Voit B. Preparation of functional poly(acrylates and methacrylates) and block copolymers formation based on polystyrene macroinitiator by ATRP. Polymer. 2005;46(10):3215-3222.
31. Vijayalakshmi SP, Madras G. Photocatalytic degradation of poly(ethylene oxide) and polyacrylamide. J Appl Polym Sci. 2006;100(5):3997-4003.
32. Scherrer P. Bestimmung der inneren Struktur und der Größe von Kolloidteilchen mittels Röntgenstrahlen. Kolloidchemie Ein Lehrbuch: Springer Berlin Heidelberg; 1912. p. 387-409.
33. Ghaziaskar HS, Xu C. One-step continuous process for the production of 1-butanol and 1-hexanol by catalytic conversion of bio-ethanol at its sub-/supercritical state. RSC Advances. 2013;3(13):4271.